Management of subcentimeter arterially enhancing and hepatobiliary hypointense lesions on gadoxetic acid-enhanced MRI in high risk patients for hepatocellular carcinoma

Chae Jung Park

Department of Medicine
The Graduate School, Yonsei University

Management of subcentimeter arterially enhancing and hepatobiliary hypointense lesions on gadoxetic acid-enhanced MRI in high risk patients for hepatocellular carcinoma

Chae Jung Park

Department of Medicine
The Graduate School, Yonsei University

Management of subcentimeter arterially enhancing and hepatobiliary hypointense lesions on gadoxetic acid-enhanced MRI in high risk patients for hepatocellular carcinoma

Directed by Professor Myeong-Jin Kim

The Master's Thesis
submitted to the Department of Medicine,
the Graduate School of Yonsei University
in partial fulfillment of the requirements for the degree
of Doctor of Philosophy

Chae Jung Park

June 2018

This certifies that the Master's Thesis of
Chae Jung Park is approved.

Thesis Supervisor : Myeong-Jin Kim

Thesis Committee Member#1 : Do Young Kim

Thesis Committee Member#2 : Chansik An

Thesis Committee Member#3: Ki Taek Nam

Thesis Committee Member#4: Jei Hee Lee

The Graduate School
Yonsei University

June 2018

ACKNOWLEDGEMENTS

I acknowledge my deep gratitude to Prof. Myeong-Jin Kim, who has been training me in abdominal radiology division, for supporting my efforts with total commitment and facilitating every step in the process of completing my thesis. My appreciation for his guidance and encouragement is tremendous.

<TABLE OF CONTENTS>

LIST OF FIGURES

LIST OF TABLES

ABSTRACT

Management of subcentimeter arterially enhancing and hepatobiliary hypointense lesions on gadoxetic acid-enhanced MRI in high risk patients for hepatocellular carcinoma

Chae Jung Park

Department of Medicine
The Graduate School, Yonsei University

(Directed by Professor Myeong-Jin Kim)

Objectives: To investigate the significance of subcentimeter (≤1 cm) arterially enhancing and hepatobiliary hypointense lesions (SAELs) observed on gadoxetic acid-enhanced magnetic resonance imaging (MRI) in high risk patients for hepatocellular carcinoma (HCC).

Methods: A SAEL was defined as a subcentimeter hypervascular nodule exhibiting a hepatobiliary phase defect on gadoxetic acid-enhanced MRI. We included 52 SAELs from 46 patients in a HCC surveillance population. The HCC reference standard was pathologic confirmation or a nodule >1 cm with typical imaging features of HCC at follow-up imaging. The malignancy rate and HCC-favorable imaging findings of SAELs were evaluated.

Results: The malignancy rate among SAELs was 57.7% (30/52). At diagnosis, all SAELs that progressed to overt HCC were treatable with curative intention. Venous or late dynamic phase washout was more frequently observed with malignant SAELs than with benign SAELs (57.7% vs. 30.6%; P = 0.01). If SAELs exhibiting washout were considered as HCC, sensitivity, specificity, and positive predictive value was 83.3%, 50%, and 69.4%, respectively.

Conclusion: Among high risk patients for HCC, SAELs on gadoxetic

acid-enhanced MRI exhibited high malignant potential. However, close observation may be an appropriate strategy for isolated SAELs. A washout appearance may be helpful for predicting malignancy.

Key words : hepatocellular carcinoma, gadoxetic acid, magnetic resonance imaging, diagnosis, sensitivity and specificity

Management of subcentimeter arterially enhancing and hepatobiliary hypointense lesions on gadoxetic acid-enhanced MRI in high risk patients for hepatocellular carcinoma

Chae Jung Park

Department of Medicine
The Graduate School, Yonsei University

(Directed by Professor Myeong-Jin Kim)

I. INTRODUCTION

Hepatocellular carcinoma (HCC) is the most common primary malignancy of the liver and the second leading cause of cancer-related mortality worldwide [1]. The early detection of HCC in high risk patients is important because therapeutic efficacy and prognosis are better in patients with early-stage HCCs than in those with advanced tumors. Dynamic contrast-enhanced liver magnetic resonance imaging (MRI) has become an essential diagnostic tool for improving the diagnosis of HCCs at earlier stages [2,3]. Hepatocyte-specific contrast agents, such as gadoxetic acid disodium, facilitate a hepatobiliary phase (HBP) that may further increase the sensitivity of MRI for diagnosing small HCCs [4,5]. However, the use of hepatocyte-specific contrast agents is one of several factors contributing to the more frequent detection of indeterminate lesions by liver MRI [6-8].

One type of indeterminate lesion identified by liver MRI is the subcentimeter (≤1 cm) arterially enhancing and hepatobiliary hypointense lesion (SAEL), which exhibits hyperenhancement in the arterial phase and hypointensity in the HBP [9,10]. The incidence of HCC among SAELs detected on gadoxetic acid-enhanced MRI is reported to be as high as 90% [9]. However, this high incidence of HCC has been reported in patients with a history of previous HCC. To our knowledge, the fates of SAEL detected in patients without a

previous HCC history have not been reported.

The purposes of our study were to evaluate the outcomes of SAELs identified during the initial imaging workups of high risk patients for HCC and to identify the MRI features that could differentiate a malignant from a benign SAEL.

II. MATERIALS AND METHODS

1. Patients

This retrospective study was approved by our Institutional Review Board, and the requirement for informed consent was waived. From September 2008 to March 2013, we searched the gadoxetic acid-enhanced MRI datasets of 2311 consecutive patients who were hepatitis B or C carriers or had received a diagnosis of liver cirrhosis, regardless of etiology, at our institute (a tertiary academic hospital). After reviewing the MRI reports and electronic medical records, we excluded 972 patients who were treated for hepatic malignancy prior to MRI (n = 697), were diagnosed with an extrahepatic primary malignancy (n = 147), had an intermediate- (n = 112) or locally advanced-stage (n = 215) of HCC 11, had a distant metastasis (n = 11) or extrahepatic vascular invasion (main portal vein and inferior vena cava) of HCC (n = 29), or had no hepatic lesion suspected of malignancy (n = 128).

Of the remaining 972 patients with early-stage HCC 11 or suspicious indeterminate nodules, one investigator (C.P., a fourth-year radiology resident) reviewed the MRI reports and identified 165 patients with at least one SAEL. A total of 182 SAELs were identified in 165 patients. Among these, 130 SAELs were excluded for the following reasons: (i) eight were satellite nodules, defined as a location $\leq$2 cm from the main HCC tumor 12; (ii) 121 were unconfirmed SAELs because of immediate transarterial chemoembolization (TACE) or local ablation without pathologic confirmation; and (iii) one SAEL was not followed up for at least 12 months. Therefore, our final sample comprised 52 SAELs from 46 patients that were confirmed to be benign lesions or HCC using the reference standard explained below (Fig. 1).

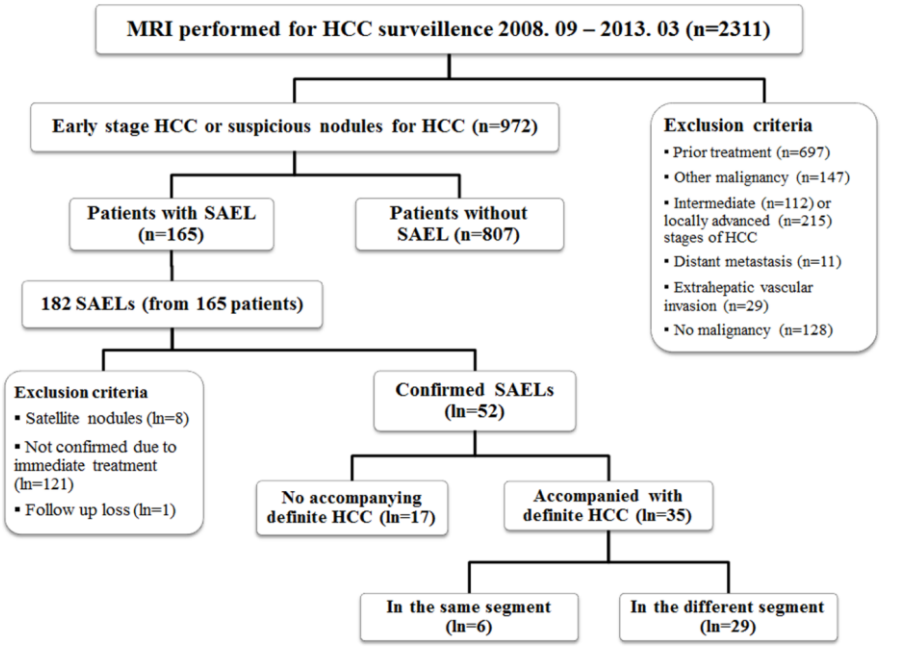

Figure 1. Flow chart shows patient characteristics and exclusion criteria (n, number of patients; ln, number of lesions).

Information about the patients' demographics, chronic liver disease etiologies, serum alpha-fetoprotein (AFP) serum levels, Child–Pugh classifications, and pathological diagnoses was obtained by reviewing the electronic medical records. One radiologist (C.P.) reviewed the MRI data from each patient with a SAEL and recorded the presence or absence of an accompanying HCC. If HCC was present, the radiologist also recorded whether the SAEL and HCC were located in the same segment.

2. Reference standard

Overt HCC was defined as a pathologically proven HCC or a SAEL >1 cm exhibiting typical imaging features of HCC (hypervascularity in the arterial phase with washout in the venous or delayed phase) on follow-up imaging. 13,14. A benign SAEL was either pathologically confirmed or considered benign if it exhibited no interval growth for ≥12 months, decreased in size, or disappeared at follow-up.

3. MRI

MRI was performed on 3.0-T systems (MAGNETOM Trio; Siemens Medical Solutions, Erlangen, Germany or Intera Achieva, Philips Medical Systems, Best, the Netherlands). After obtaining localizer images, two-dimensional, dual-echo T1-weighted gradient-recalled echo images were obtained with a slice thickness, intersection gap, and repetition time (TR) of 7 mm, 0.7 mm, and 150–192 msec, respectively. The echo times (TEs) for in-phase and opposed-phase images were 2.3–2.46 and 1.14–1.23 msec, respectively. Pre- and post-contrast dynamic images, including arterial, venous, late dynamic, and hepatobiliary phase, were subsequently obtained using a three-dimensional gradient echo sequence with a section thickness, TR, and TE of 2–4 mm, 2.54–4.48 msec, and 0.92–2.2 msec, respectively. To determine the scan delay for arterial phase imaging, a bolus technique was used with 1 mL gadoxetic acid disodium (Primovist; Bayer Schering Pharma, Berlin, Germany) or bolus-tracking images were obtained to determine the peak enhancement of the abdominal aorta. For dynamic imaging, a fixed 10-mL dose of gadoxetic acid disodium was injected, followed by 20 mL of 0.9% saline at an injection rate of 1 or 2 mL/s. The arterial phase began 2–3 sec after peak aortic enhancement, which was calculated using the test bolus technique, or after the bolus of contrast material reached the abdominal aorta; subsequent dynamic images were obtained at intervals of approximately 30 sec. Each dynamic image acquisition required 16–22 sec. Hepatobiliary images were obtained 15 or 20 min after contrast agent injection, using the same imaging sequence used for the pre- and post-contrast images. During the interval between dynamic and HBP imaging, T2-weighted images (T2WI) were obtained using multi-shot and single-shot turbo-spin echo sequences and a navigator-triggered technique with a section thickness, gap, TR, and TE of 5–7 mm, 1 mm, 1589–3250 msec, and 70–96 msec, respectively. Diffusion-weighted images (DWI) were obtained using a navigator-triggered technique at b-values of 50, 400, and 800 sec/mm2. The apparent diffusion coefficient (ADC) was automatically calculated by the MRI devices and displayed as a corresponding ADC map.

4. Image analysis

MRI data were retrieved from a local picture archiving and communication system (Centricity, Version 2.0, GE Healthcare, Barrington, IL, US). During a review of the MRI images with pathology reports and surgery records, one radiologist (C.P.) recorded and marked the sizes and locations (hepatic segment) of SAELs on maps according to the Couinaud system of liver anatomy. The nodule size was recorded as the longest diameter measured in the transverse plane of HBP. The MRI data were subsequently de-identified and presented in random order to two board-certified abdominal radiologists (S.P. and C.A., with 16 and 6 years of experience with liver MRI interpretation, respectively) with the maps on which the size and location of each SAEL were marked. The two radiologists performed independent image analysis and then met to draw final conclusions on discordant cases by consensus. The radiologists were blinded to the final diagnosis and clinical information, but were aware that the patients were at a high risk of HCC development. For each nodule, they determined the presence or absence of washout appearance in the venous or late dynamic phase, capsule appearance, intralesional fat, and signal intensities (SI) on T2WI and DWI using definitions from the 2014 version of the Liver Imaging Reporting and Data System (LI-RADS) 15.

We calculated sensitivity and specificity for HCC diagnosis by applying two noninvasive diagnostic criteria, where diagnosis of subcentimeter HCC was feasible by imaging. According to the Liver Cancer Study Group of Japan (LCSGJ) 16, subcentimeter lesions can be diagnosed as HCC if they exhibit arterial hypervascularity and hepatobiliary hypointensity on hepatobiliary phase imaging. According to the Korean Liver Cancer Study Group and the National Cancer Center (KLCSG-NCC) guidelines 17, a noninvasive diagnosis of HCC can be made for SAELs exhibiting a radiological hallmark on two or more imaging modalities along with a trend toward increasing serum AFP levels over time. Diagnostic accuracy for HCC diagnosis among SAELs was also calculated by combining other imaging findings, such as venous or late dynamic phase washout, diffusion restriction, and hyperintensity on T2WI. We

also reviewed the follow-up results of patients who did not immediately receive treatment after SAEL detection to assess the appropriateness of a wait-and-see approach for these lesions.

5. Statistical analysis

Differences in the frequencies of imaging features among HCCs and benign SAELs were compared using Fisher's exact test or the chi-square test. Differences in tumor sizes and serum AFP levels were compared using Student's t-test. The degree of agreement between the two radiologists was calculated using the Kappa statistic test. A kappa statistic of 0.8–1 was considered excellent, 0.6–0.79 was good, 0.4–0.59 was moderate, 0.2–0.39 was fair and 0–0.19 was poor agreement. Two-sided P-values of <0.05 were considered statistically significant. Data were analyzed using commercially available statistics software (SAS 9.2; SAS Institute Inc., Cary, NC, USA).

III. RESULTS

1. Patient demographics

The baseline characteristics of 46 patients with 52 SAELs are presented in Table 1. Hepatitis B-viral infection was the most common etiology of underlying liver disease (37/46, 80.4%). A majority of patients exhibited imaging features of liver cirrhosis (34/46, 73.9%). All but three patients were classified as Child–Pugh A (93.5%, 43/46). The serum AFP levels were within normal limits (<9 ng/L) in 20 (43.5%) patients and elevated in 26 (56.5%) patients.

Table 1. Characteristics of the study population

Baseline characteristics	Number of patients
Male:Female ratio	41:5
Age (years)[1]	57.1 ± 9.1
Etiology of liver disease	
B-viral liver cirrhosis	27 (58.7%)
C-viral liver cirrhosis	5 (10.9%)
B and C-viral liver cirrhosis	1 (2.2%)
Alcoholic liver cirrhosis	1 (2.2%)
Non-B and non-C liver cirrhosis	3 (6.5%)
Chronic B-viral hepatitis	9 (19.6%)
Child-Pugh class	
Class A	43 (93.5%)
Class B	3 (6.5%)
Serum AFP level (ng/L)[2]	10.1 (1.6–4715.7)
Normal (<9 ng/mL)	20 (43.5%)
9-200	21(45.6%)
>200	5 (10.9%)

[1] Data are mean ± standard deviation

[2] Data are medians with range in parentheses.

SAEL: arterially enhancing and hepatobiliary hypointense lesion, AFP: alpha-fetoprotein

2. Imaging and clinical features of 52 confirmed SAELs

Of the 52 confirmed SAELs, 30 (57.7%) were diagnosed as HCC. Twenty-five HCCs and 16 benign nodules were confirmed pathologically, and five HCCs and six benign nodules were diagnosed by imaging follow-up. The 16 pathologically confirmed benign lesions received the following diagnoses: 12 dysplastic nodules, two eosinophilic abscesses, one bile duct adenoma, and one Von Meyenburg complex. For the 25 pathologically confirmed HCCs, the median interval between MRI and surgical treatment was 15 days (range, 1–224

days). The mean nodule size did not differ significantly between the benign and HCC groups (7.8 mm and 8.2 mm, respectively; P = 0.421). The presence of accompanying HCC was not significantly associated with a final diagnosis of SAEL (P = 0.999). Seventeen SAELs were not accompanied by HCC at the time of diagnosis, whereas 35 were detected with accompanying HCCs in the same (n = 6) or different hepatic segments (n = 27). Among the 17 SAELs without accompanying HCC, 10 (58.8%) were diagnosed as HCC. Of the 35 SAELs accompanied by HCC, 20 (57.1%) were diagnosed as HCCs. The progression rate to HCC did not differ significantly between SAELs with and without accompanying HCC. In the group with accompanying HCC, the malignant SAELs were more frequently detected in the same segment as HCC, compared with benign SAELs (25% vs. 6.7%), although this difference was not significant (P = 0.207).

When the MRI features of HCC and benign SAELs were compared, a venous or late dynamic phase washout appearance was the only imaging finding that was more frequently observed in the HCC group relative to the benign group with statistical significance (83.3% vs. 50.0%; P = 0.01) (Figures 2 and 3) (Table 2). No other imaging features (T2 SI, diffusion restriction, capsule appearance, and intralesional fat) differed significant in frequency between the two groups. The interobserver agreement regarding the presence of a washout appearance, which was significantly associated with malignancy, was good (k = 0.662). The interobserver agreements regarding the other imaging features varied from moderate to excellent (k = 0.940 for T2 SI, k = 0.846 for DWI, k = 0.625 for the presence of capsule appearance and k = 0.559 for presence of intralesional fat).

Figure 2. A subcentimeter arterially enhancing hepatobiliary hypointense lesion (SAEL) confirmed as a hepatocellular carcinoma (HCC) in an 84-year-old man with a chronic hepatitis C viral infection. Axial dynamic contrast-enhanced T1-weighted images revealed a subcentimeter nodule in S7 of the liver. This nodule exhibited hyperenhancement in the arterial phase (a), washout appearance in the venous phase (b), and hypointensity in the hepatobiliary phase (c). The 3-month follow-up MRI revealed an increase in SAEL size from 1.0 cm to 1.6 cm (d), leading to a diagnosis of HCC. Subsequent radiofrequency ablation was performed.

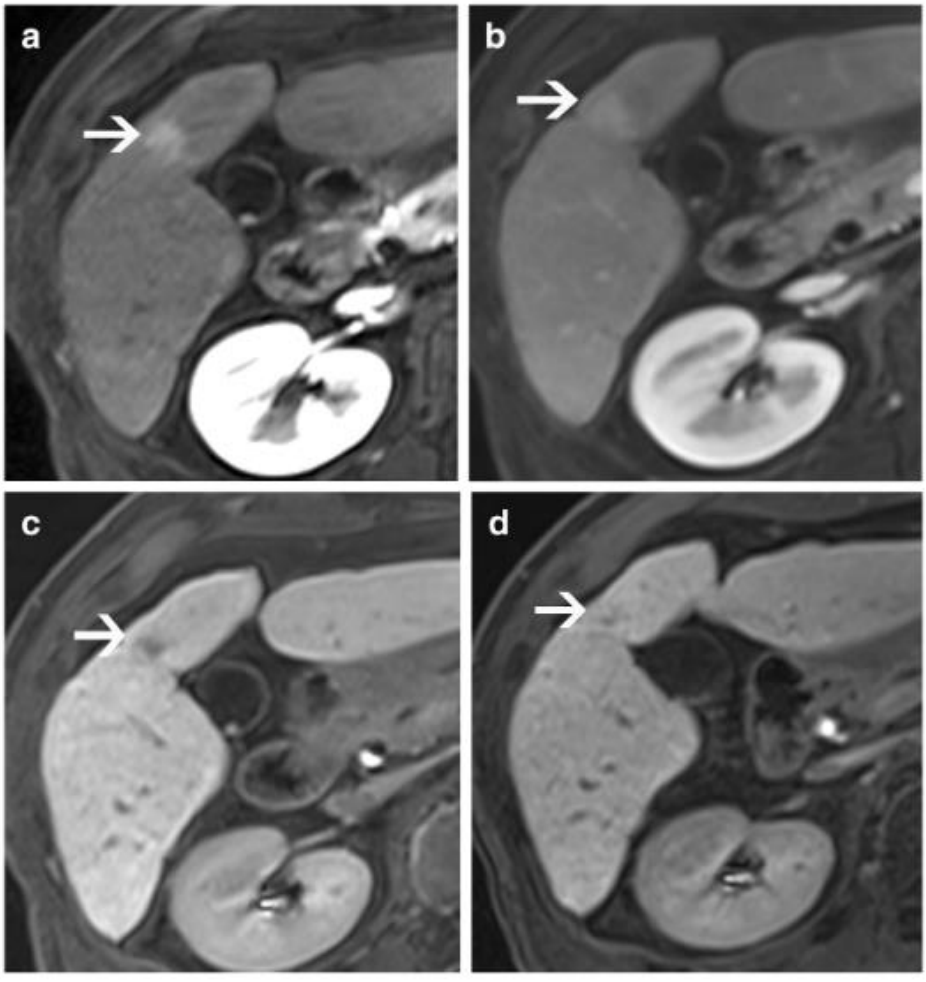

Figure 3. A subcentimeter arterially enhancing hepatobiliary hypointense lesion (SAEL) in a 70-year-old man with a hepatitis C viral infection. Axial dynamic contrast-enhanced T1-weighted images revealed a subcentimeter nodule in S4 of the liver. This nodule exhibited hyperenhancement in the arterial phase (a) without washout appearance in venous phase (b), and showed hypointensity in the hepatobiliary phase (c). At the 2-month follow-up, the SAEL had nearly disappeared (d) and was diagnosed as a benign lesion.

Table 2. Imaging features of 52 confirmed SAELs

	Benign	Malignant	*P* value
Total number of lesions	22	30	
Longest diameter (mm)*	7.8 ± 1.9	8.2 ± 1.6	0.421
Accompanying HCC			0.999
Absent	7 (31.8%)	10 (33.3%)	
Present in the same segment as SAEL	1(4.5%)	5 (16.7%)	
Present in different segments	14 (63.6%)	15 (50%)	
Washout appearance			0.01
Yes	11 (50%)	25 (83.3%)	
No	11 (50%)	5 (16.7%)	
T2 signal intensity			0.355
High	16 (72.7%)	25 (83.3%)	
Iso	6 (27.3%)	5 (16.7%)	
Diffusion restriction			0.376
Yes	9 (40.9%)	16 (53.3%)	
No	13 (59.1%)	14 (46.7%)	
Presence of capsule appearance			0.999
Yes	2 (9.1%)	2 (6.7%)	
No	20 (90.9%)	28 (93.3%)	
Presence of intralesional fat			0.685
Yes	2 (9.1%)	5 (16.7%)	
No	20 (90.9%)	25 (83.3%)	
Serum AFP			
All SAELs (ng/L)†	3.6 (1.6–250.3)	12.7 (1.6–4715.7)	0.038
Normal (<9 ng/L)	15 (68.2%)	12 (40%)	0.044
Elevated	7 (31.8%)	18 (60%)	
Isolated SAELs‡ (ng/L)†	2.2 (1.8–215.3)	6.4 (1.6–327.2)	0.143

Normal (<9 ng/L)	6 (85.7%)	6 (60%)	0.338
Elevated	1 (14.3%)	4 (40%)	

[1]Data are shown as mean and standard deviation

[2]Data are median with range in parentheses

[3]SAELs without accompanying HCC

SAEL: subcentimeter arterial enhancing hepatobiliary hypointense lesions, HCC: hepatocellular carcinoma, AFP: alpha-fetoprotein

The serum AFP levels were significantly higher in HCCs compared to those in benign SAELs (median, 12.7 ng/L vs. 3.6 ng/L; P = 0.038). In the group without accompanying HCC, serum AFP level was higher (median, 6.4 ng/L vs. 2.2 ng/L; P = 0.143) and more frequently elevated (>9 ng/L, 40% vs. 14.3%; P = 0.338) in the HCC group compared to the benign group; however, these differences were not statistically significant.

3. Accuracy of radiologic diagnosis for HCC among SAELs

The diagnostic performances of various noninvasive diagnostic criteria for HCC were evaluated (Table 3). According to the LCSGJ [16], all SAELs would be diagnosed as HCC, thus, positive predictive value was 57.7% (32/50). Because the KLCSG-NCC requires the use of two or more imaging modalities or an increasing trend in serum AFP levels over time for the diagnosis of HCC [17], this guideline was applicable to only 18 SAELs resulting in a sensitivity of 28.6% (2/7) and specificity of 90.1% (10/11).

Table 3. Diagnostic performance of various noninvasive imaging criteria for HCC diagnosis

	Sensitivity	Specificity
Liver Cancer Study Group of Japan (LCSGJ)	100%	0%
Korean Liver Cancer Study Group and the National Cancer Center (KLCSG-NCC) guideline	28.6%	90.1%
SAEL + Washout appearance	83.3%	50%
SAEL + T2 high SI or diffusion restriction	83.3%	27.3%
SAEL + Washout appearance + T2 high SI or diffusion restriction	73.3%	63.6%

HCC: hepatocellular carcinoma, SAEL: subcentimeter arterial enhancing hepatobiliary hypointense lesions, SI: signal intensity

The diagnostic accuracy for the differentiation of SAEL was calculated by combining other imaging findings (Table 3). For the diagnosis of HCC, a SAEL exhibiting venous or late dynamic phase washout appearance yielded a sensitivity, specificity, and positive predictive value of 83.3%, 50%, and 69.4%, respectively. When SAELs demonstrating either moderate high SI on T2WI or diffusion restriction were considered HCC, sensitivity for HCC diagnosis did not change (83.3%), but specificity decreased to 27.3%. When both the washout appearance and either a moderate T2 high SI or diffusion restriction were used as diagnostic criteria for HCC, the specificity increased to 63.6%, but the sensitivity decreased to 73.3%.

We also reviewed the follow-up outcomes of 11 SAELs for which treatment was not performed immediately after the initial examination to assess the appropriateness of a wait-and-see approach for these lesions (Table 4). Of these 11 SAELs, five (45%) progressed to HCCs in four patients. All five HCCs were diagnosed with diameters of <2 cm on follow-up examinations, without the

development of other HCCs in the remaining liver. Therefore, treatment was not considered to be delayed.

Table 4. Natural histories of 11 SAELs followed up without immediate treatment

Sex/age	Time to diagnosis (months)	Initial size (mm)	Size at diagnosis (mm)	Accompanying HCC	Final diagnosis	Treatment
M/63	24	10	16	Yes (different segments)	HCC	TACE
M/84	3	10	16	None	HCC	RFA
M/63	6	9	12	None	HCC	TACE
M/63	6	9	12	None	HCC	TACE
M/66	3	7	13	None	HCC	TACE
M/56	48	5	5	Yes (different segments)	Benign	NA
M/58	3	10	disappeared	Yes (different segments)	Benign	NA
M/62	2	10	disappeared	None	Benign	NA
M/63	3	10	disappeared	None	Benign	NA
M/52	12	7	7	None	Benign	NA
F/60	24	8	8	None	Benign	NA

HCC: hepatocellular carcinoma, SAEL: subcentimeter arterial enhancing hepatobiliary hypointense lesions, NA: not applicable, TACE: transarterial chemoembolization, RFA: radiofrequency ablation

IV. DISCUSSION

In our study, 30 (57.7%) of 52 SAELs were finally confirmed as HCC, and a venous or late dynamic phase washout appearance was the only MRI finding that was significantly associated with malignancy in these lesions. However, a washout appearance was also frequently observed in benign SAELs, suggesting that the differentiation of benign and malignant subcentimeter nodules based on imaging findings alone is challenging. Although several authoritative guidelines recommend imaging follow-ups of subcentimeter

nodules [13,14], it remains uncertain whether this is the most appropriate and practical diagnostic method for SAELs. In a group of 10 patients with 11 SAELs in our study who were followed up without immediate diagnosis or treatment, five HCCs were diagnosed in four patients after 3–24 months of follow-up. However, none of these patients experienced tumor stage progression during the follow-up period. Even though the number of cases was small, a close follow-up with a short-term interval (e.g., 3 months) might be appropriate for the management of SAELs identified on gadoxetic acid-enhanced MRI without losing the opportunity for timely treatment [13, 14].

Song et al. assessed the natural courses of subcentimeter hypervascular and hepatobiliary hypointense nodules identified on gadoxetic acid-enhanced MRI [9]. The authors reported a cumulative progression rate to overt HCC of 89.9% at 12 months, which was higher than the rate (57.7%) in our study. However, the higher progression rate to overt HCC in this earlier study can be attributed to the enrollment of patients with a history of previous treatment for HCC, and we note that these patients were excluded from our study. In addition, the previous study included only subcentimeter hypervascular and hepatobiliary hypointense nodules exhibiting additional hallmarks of HCC including venous phase washout appearance, moderately high SI on T2WI and diffusion restriction, and this also likely contributed to the higher rate of progression to HCC. Similarly, in our study, among 16 SAELs exhibiting all diagnostic hallmarks of HCC (venous or late dynamic washout appearance, moderately high SI on T2WI, and diffusion restriction), 13 (81.3%) were confirmed as HCCs. This result suggests that even in the absence of a previous history of HCC, subcentimeter nodules exhibiting all diagnostic hallmarks of HCCs are highly likely to progress to HCC in high-risk patients.

Our results demonstrate that the KLCSG-NCC guidelines are highly specific for HCC diagnosis. However, these guidelines were not applicable to all patients in our study population because they are intended to be applied to lesions detected initially on US surveillance, and a noninvasive diagnosis of HCC for such nodules requires an increasing trend in the serial AFP levels and

positive findings on at least two imaging modalities. However, none of the SAELs in our study were detected on previous US. In contrast, when the LCSGJ guidelines were applied to our series, all SAELs were diagnosable as HCCs, yielding a positive predictive value of only 57.7% (32/50). This result suggests that even among super high-risk patients, the current LCSGJ guidelines might lead to a high false-positive diagnosis rate of HCC among SAELs.

Our study had several limitations. First, our retrospective study design may have introduced selection bias, as many SAELs were subjected to immediate TACE or local ablation without pathological confirmation mainly because of accompanying HCC. Second, not all lesions were histopathologically confirmed. However, a substantial portion of SAELs were pathologically confirmed (78.8%), and the remaining 11 SAELs were separately reviewed to assess the appropriateness of a wait-and-see policy. Third, SAELs with mean diameters of 5–8 mm were analyzed at section thicknesses of 5–7 mm on T2WI and 5 mm on DWI. Therefore, partial volume effects might have influenced the results for comparing progression to HCC between these and larger lesions.

V. CONCLUSION

In conclusion, SAELs observed on gadoxetic acid-enhanced MRI in high risk patients for HCC were found to exhibit a strong potential for malignancy. However, close observation may be an appropriate strategy for isolated SAELs. A washout appearance may be helpful for diagnosing malignant SAELs.

REFERENCES

1. Mittal S, El-Serag HB. Epidemiology of hepatocellular carcinoma: consider the population. J Clin Gastroenterol 2013;47 Suppl:S2-6.
2. Lee YJ, Lee JM, Lee JS, Lee HY, Park BH, Kim YH, et al. Hepatocellular carcinoma: diagnostic performance of multidetector CT and MR imaging-a systematic review and meta-analysis. Radiology 2015;275:97-109.
3. Kim HD, Lim YS, Han S, An J, Kim GA, Kim SY, et al. Evaluation of early-stage hepatocellular carcinoma by magnetic resonance imaging with gadoxetic acid detects additional lesions and increases overall survival. Gastroenterology 2015;148:1371-82.
4. Ahn SS, Kim MJ, Lim JS, Hong HS, Chung YE, Choi JY. Added value of gadoxetic acid-enhanced hepatobiliary phase MR imaging in the diagnosis of hepatocellular carcinoma. Radiology 2010;255:459-66.
5. Bashir MR, Gupta RT, Davenport MS, Allen BC, Jaffe TA, Ho LM, et al. Hepatocellular carcinoma in a North American population: does hepatobiliary MR imaging with Gd-EOB-DTPA improve sensitivity and confidence for diagnosis? J Magn Reson Imaging 2013;37:398-406.
6. Rosenkrantz AB, Pinnamaneni N, Kierans AS, Ream JM. Hypovascular hepatic nodules at gadoxetic acid-enhanced MRI: whole-lesion hepatobiliary phase histogram metrics for prediction of progression to arterial-enhancing hepatocellular carcinoma. Abdom Radiol (NY) 2016;41:63-70.
7. Motosugi U, Bannas P, Sano K, Reeder SB. Hepatobiliary MR contrast agents in hypovascular hepatocellular carcinoma. J Magn Reson Imaging 2015;41:251-65.
8. Hyodo T, Murakami T, Imai Y, Okada M, Hori M, Kagawa Y, et al. Hypovascular nodules in patients with chronic liver disease: risk factors for development of hypervascular hepatocellular carcinoma. Radiology 2013;266:480-90.

9. Song KD, Kim SH, Lim HK, Jung SH, Sohn I, Kim HS. Subcentimeter hypervascular nodule with typical imaging findings of hepatocellular carcinoma in patients with history of hepatocellular carcinoma: natural course on serial gadoxetic acid-enhanced MRI and diffusion-weighted imaging. Eur Radiol 2015;25:2789-96.
10. Jang KM, Kim SH, Kim YK, Choi D. Imaging features of subcentimeter hypointense nodules on gadoxetic acid-enhanced hepatobiliary phase MR imaging that progress to hypervascular hepatocellular carcinoma in patients with chronic liver disease. Acta Radiol 2015;56:526-35.
11. Yau T, Tang VYF, Yao T-J, Fan S-T, Lo C-M, Poon RTP. Development of Hong Kong Liver Cancer Staging System With Treatment Stratification for Patients With Hepatocellular Carcinoma. Gastroenterology 2014;146:1691-700.e3.
12. Roayaie S, Blume IN, Thung SN, Guido M, Fiel MI, Hiotis S, et al. A system of classifying microvascular invasion to predict outcome after resection in patients with hepatocellular carcinoma. Gastroenterology 2009;137:850-5.
13. European Association For The Study Of The L, European Organisation For R, Treatment Of C. EASL-EORTC clinical practice guidelines: management of hepatocellular carcinoma. J Hepatol 2012;56:908-43.
14. Bruix J, Sherman M. Management of hepatocellular carcinoma: an update. Hepatology 2011;53:1020-2.
15. American College of Radiology. Liver Imaging Reporting and Data System version 2014. Accessed Month 2016, from http://www.acr.org/Quality-Safety/Resources/LIRADS. .
16. Kudo M, Matsui O, Izumi N, Iijima H, Kadoya M, Imai Y, et al. Surveillance and diagnostic algorithm for hepatocellular carcinoma proposed by the Liver Cancer Study Group of Japan: 2014 update. Oncology 2014;87 Suppl 1:7-21.
17. Lee JM, Park JW, Choi BI. 2014 KLCSG-NCC Korea Practice

Guidelines for the Management of Hepatocellular Carcinoma: HCC Diagnostic Algorithm. Digestive Diseases 2014;32:764-77.

ABSTRACT(IN KOREAN)

간세포암종 고위험군 환자의 Gadoxetate 조영증강 자기공명영상에서 관찰되는 1cm 미만의 과혈관성 병변의 치료방침

<지도교수 김명진>

연세대학교 대학원 의학과

박 채 정

목적: 간세포암종의 고위험군 환자를 대상으로 간세포 특이적 조영제를 사용하여 시행한 자기공명영상에서 발견되는 1cm 미만의 과혈관성이면서 간담도기에서 낮은 신호를 보이는 병변 (Subcentimeter arterially enhancing and hepatobiliary hypointense lesion, SAELs)의 임상적 의미를 알아보고자 하였다.

방법: 1cm 미만의 과혈관성이면서 간담도기에서 낮은 신호를 보이는 병변을 'SAEL'이라고 명칭하였다. 검진 목적으로 자기공명영상을 시행한 간세포암종의 고위험군 환자들 가운데에 총 46명의 환자로부터 52개의 SAEL을 발견하였다. 연구의 대상이 된 52개의 SAEL의 영상 소견 및 의무기록을 확인하여, 조직학적으로 간세포암종이 진단되거나 영상으로 추적 관찰하였을 때 병변의 크기가 1cm 이상으로 커지면서 동시에 간세포암종의 전형적인 소견을 보이게 된 경우에 간세포암종으로 진단하였다. SAEL 중 간세포암종으로 진단되는 백분율을 계산하였고, 간세포암종을 시사하는 영상소견을 알아보고자 하였다.

결과: SAEL 중 간세포암종으로 진단된 백분율은 57.7% (30/52)였다. 30개의 SAEL이 간세포암종으로 진단될 당시 모든 SAEL은 완치 목적의 치료가 가능하였다. 자기공명영상 정맥기에서 저신호로 보이는 소견은 양성 SAEL보다 악성 SAEL에서 더 흔하게 관찰되었으며 이 차이는 통계학적으로 유의미하였다 (57.7% vs. 30.6%; P = 0.01). 정맥기에서 저신호를 보이는 SAEL을 간세포암종으로 진단하였을 때, 민감도, 특이도 및 양성예측치는 각각

83.3%, 50%, 그리고 69.4%로 나타났다.

결론: 간세포암종의 고위험군 환자를 대상으로 간세포 특이적 조영제를 사용하여 시행한 자기공명영상에서 발견되는 SAEL은 절반 이상의 높은 악성화 가능성을 보였다. 그러나, 간세포암종으로 밝혀진 모든 SAEL이 진단 당시에 암의 병기가 더 진행하지 않았다는 점에서, 이를 즉각 치료하는 것보다 주의 깊은 추적관찰을 시행하는 것은 적절한 대처일 수 있다고 판단하였다. 자기공명영상 정맥기에서 저신호 강도를 보이는 소견은 악성을 예측하는 데에 도움을 줄 수 있다.

핵심되는 말 : 간세포암종, 가돌리늄조영제, 자기공명영상, 진단, 민감도, 특이도

PUBLICATION LIST

1. Park CJ, An C, Park S, Choi JY, Kim MJ. Management of subcentimetre arterially enhancing and hepatobiliary hypointense lesions on gadoxetic acid-enhanced MRI in patients at risk for HCC: Eur Radiol 2018;28(4):1476-84.